Journal of Materials Chemistry A

Accepted Manuscript

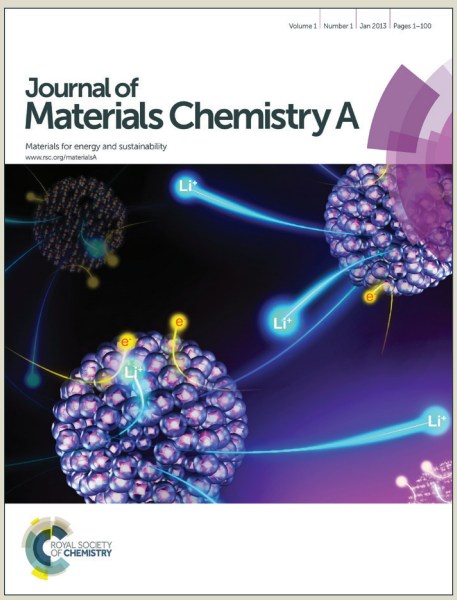

This is an *Accepted Manuscript*, which has been through the Royal Society of Chemistry peer review process and has been accepted for publication.

Accepted Manuscripts are published online shortly after acceptance, before technical editing, formatting and proof reading. Using this free service, authors can make their results available to the community, in citable form, before we publish the edited article. We will replace this *Accepted Manuscript* with the edited and formatted *Advance Article* as soon as it is available.

You can find more information about *Accepted Manuscripts* in the Information for Authors.

Please note that technical editing may introduce minor changes to the text and/or graphics, which may alter content. The journal's standard Terms & Conditions and the Ethical guidelines still apply. In no event shall the Royal Society of Chemistry be held responsible for any errors or omissions in this *Accepted Manuscript* or any consequences arising from the use of any information it contains.

ROYAL SOCIETY OF CHEMISTRY

www.rsc.org/materialsA

Journal of Materials Chemistry A RSCPublishing

ARTICLE

Application of pyrene-derived benzimidazole-linked polymers to CO_2 separation under pressure and vacuum swing adsorption settings

`Cite this: DOI: 10.1039/x0xx00000x

Received 00th March 2014,
Accepted 00th March 2014

DOI: 10.1039/x0xx00000x

www.rsc.org/

Ali Kemal Sekizkardes, Timur İslamoğlu, Zafer Kahveci and Hani M. El-Kaderi*

Pyrene-derived benzimidazole-linked polymers (BILPs) have been prepared and evaluated for selective CO_2 uptake and separation under pressure and vacuum swing conditions. Condensation of 1,3,6,8-tetrakis(4-formylphenyl)pyrene (TFPPy) with 3,6,7,10,11-hexaaminotriphenylene, 2,3,6,7,14,15 hexaaminotriptycene, and 3,3`diaminobenzidine afforded BILP-11, BILP-12 and BILP-13, respectively, in good yields. BILP-12 exhibits the highest specific surface area (SA_{BET} = 1497 $m^2 g^{-1}$) among all known BILPs and it also has very high CO_2 uptake 5.06 mmol g^{-1} at 273 K and 1.0 bar. Initial slope selectivity calculations indicate that BILP-11 has high selectivity for CO_2/N_2 (103) and CO_2/CH_4 (11) at 273 K. IAST selectivity calculations of BILPs at 298 K also showed high CO_2/N_2 (31-56) and CO_2/CH_4 (6.6-7.6) selectivity levels. The isosteric heats of adsorption for CO_2 fall in the range of 32 to 36 kJ mol^{-1} and were considerably higher than those of CH_4 (16.1-21.7 kJ mol^{-1}). More importantly, the performance of pyrene-based BILPs in CO_2 removal from flue gas and methane–rich gases (natural gas and landfill gas) under different industrial conditions was investigated according to evaluation criteria suggested recently by Bae and Snurr. The outcome of this study revealed that BILPs are among the best known porous materials in the field; they exhibit high working capacity, regenerability, and sorbent selection parameters. Collectively, these properties coupled with the remarkable physicochemical stability of BILPs make this class of polymers very promising for CO_2 separation applications.

1. Introduction

Recently there has been considerable interest in the development of porous adsorbents for carbon capture and sequestration (CCS); a process needed to mitigate climate change. With the continuous use of fossil-based fuels that account for about 87% of the world's energy, the release of CO_2 to the atmosphere will keep increasing unless CCS processes become widely employed at an affordable cost.[1-3] While amine-solutions like monoethanolamine (MEA, 30 wt% in water) are commonly used for CO_2 capture from flue gas of coal-fired plants, these solvents exhibit several challenges that make them less desirable.[2, 4] The most challenging aspect of using MEA solutions is regeneration processes which consume about 40% of the output of plants, not to mention their chemical instability, volatility, and corrosive nature.[2, 5] Because CO_2 reacts with amines to form carbamate, the release of CO_2 requires intensive energy and as such elevating this drawback can be addressed by the use of alterative adsorbents that capture CO_2 physically and release it without energy input as in the case of porous solids.[6, 7] Alternatively, porous adsorbents are emerging as new candidates for CO_2 capture because of their high porosity, tunable pore metrics, and high CO_2 uptake properties.[8] Tailoring the chemical and physical properties of porous adsorbents to make them suitable for CO_2 capture from flue gas has been proven essential as these physicochemical properties are central to effective CO_2 capture and separation processes.[9-12] For example, Wilmer *et al.*[13] have screened over 130,000 structures of metal-organic frameworks (MOFs) and identified the chemical and structural properties of MOFs that are relevant to CO_2 capture from flue gas and methane-rich gases (i.e. natural gas and landfill gas). Furthermore, the study related structural features of adsorbents to separation processes; vacuum and pressure swing methods. These processes were selected over temperature swing because the latter is less applicable as it consumes considerable energy.

Although numerous porous organic and organic-inorganic hybrid materials have been evaluated for CO_2 capture and separation, only a very limited number were investigated under vacuum (VSA) and pressure swing adsorption (PSA) settings. The general observation made by Bae and Snurr was that high surface area property favors CO_2 separation from landfill gas in PSA, whereas narrow pore size and high enthalpies of adsorption lead to optimal CO_2 removal from flue gas using VSA. Furthermore, five evaluation criteria (Table 1) were adopted from the chemical engineering field to investigate the effectiveness of porous adsorbents: CO_2 uptake, working capacity for CO_2, adsorbent regenerability, selectivity under

Journal of Materials Chemistry A Accepted Manuscript

adsorption conditions, and sorbent selection parameter. These criteria, although not perfect, provide a more comprehensive approach for assessing the suitability of porous adsorbents in CCS processes.[14]

Very recently several studies have attempted addressing such challenges by developing benzimidazole-linked polymers (BILPs), which possess high surface area and chemical stability in addition to N-functionalized pore walls.[15-17] Collectively, these properties enable high CO_2 uptake and selectivity over CH_4 and N_2, and isosteric heats of adsorption in the range of 27 to 38 kJ mol^{-1},[16, 17] which make BILPs ideal for CO_2 separation from flue gas and landfill gas using PSA or VSA. In this study we report the synthesis of porous pyrene-derived BILPs and use the five criteria discussed above to demonstrate the remarkable performance of BILPs in CO_2 capture and separation from N_2 and CH_4 under VSA and PSA conditions. We show that the performance of the reported BILPs in CO_2/N_2 and CO_2/CH_4 separations is among the best in the field of porous organic and inorganic-organic hybrid materials, which make BILPs very attractive candidates for CO_2 capture and separation applications.

Table 1. Adsorbent evaluation criteria suggested by Bae and Snurr.[14]

CO_2 uptake under adsorption conditions (mol kg^{-1})	N_1^{ads}
Working CO_2 capacity (mol kg^{-1}), $N_1^{ads} - N_1^{des}$	ΔN_1
Regenerability (%), $(\Delta N_1/N_1^{ads})x100$	R
Selectivity under adsorption conditions, $(N_1^{ads}/N_2^{ads})x(y_2/y_1)$	α_{12}^{ads}
Sorbent selection parameter, $(\alpha_{12}^{ads})^2/(\alpha_{12}^{des})x\ (\Delta N_1/\Delta N_2)$	S

N: adsorbed amount, y: molar fraction in the bulk phase. Subscripts 1 and 2 correspond to the strongly adsorbed component (CO_2) and the weakly adsorbed component (CH_4 or N_2), respectively. α_{12} : Selectivity of gas component 1 over 2. ads and des correspond to adsorption and desorption conditions, respectively.

2. Experimental Section

2.1. General techniques, materials, and methods. All chemicals were purchased from commercial suppliers (Sigma-Aldrich, Acros Organics and Frontier Scientific) and used without further purification, unless otherwise noted. 3,3`diaminobenzidine was purchased from Acros Organics. 2,3,6,7,10,11-hexaaminotriphenylene (HATP),[15] and 2,3,6,7,14,15-hexaaminotriptycene (HATT),[18] were synthesized using reported procedure. Air-sensitive samples and reactions were handled under an inert atmosphere of nitrogen using either glovebox or Schlenk line techniques. Chromatographic separations were performed using standard flash column chromatography methods using silica gel (60 Å, 35-70 µm). Elemental microanalyses were performed at the Midwest Microlab, LLC. ^{1}H and ^{13}C NMR spectra were obtained on a Varian Mercury-300 MHz NMR spectrometer. ^{13}C cross-polarization magic angle spinning (CPMAS) NMR spectra for solid samples were taken at Spectral Data Services, Inc. Thermogravimetric analysis (TGA) were carried out using a TA Instruments Q-5000IR series thermal gravimetric analyser with samples held in 50 µL platinum pans under atmosphere of air (heating rate 5 °C/min). For Scanning Electron Microscopy Imaging (SEM), sample was prepared by dispersing the material onto a sticky carbon surface attached to a flat aluminium sample holder. The sample was then coated with platinum at $7x10^{-5}$ mbar of pressure in a nitrogen atmosphere for 50 seconds before imaging. Images were taken on a Hitachi SU-70 Scanning Electron Microscope. Powder X-ray diffraction data were collected on a Panalytical X'pert pro multipurpose diffractometer (MPD). Samples were mounted on a sample holder and measured using Cu Kα radiation with a 2θ range of 1.5-35. FT-IR spectra were obtained as KBr pellets using Nicolet-Nexus 670 spectrometer. Sorption experiments were run using a Quantachrome Autosorb 1-C analyser. High pressure gas sorption measurements were performed by using VTI-HPVA-100 volumetric analyser. High pressure total gas uptakes were calculated by reported literature methods and NIST Thermochemical Properties of Fluid Systems were applied to the calculations.[17, 19]

2.2 Synthesis of Polymers

Synthesis of BILP-11. A 250 mL Schlenk flask was charged with 3,6,7,10,11-hexaaminotriphenylene hexahydrochloride salt (58 mg, 0.11 mmol), 70 mL of anhydrous DMF, and a stir-bar. The resultant homogeneous solution was cooled to -30 °C and treated with TFPPy (50 mg, 0.08 mmol) dropwise dissolved in anhydrous DMF (115 mL). The temperature was maintained around -30 °C for 6 hours during which a brown solid formed then the resultant slurry solution was allowed to warm to room temperature overnight. The flask containing the reaction mixture was flushed with air for 20 minutes and capped tightly. The reaction mixture was then transferred to a static oven and heated gradually to 130 °C (0.5 °C/min) and kept for 3 days to afford a fluffy yellow powder. The solid was isolated by filtration over a medium glass frit and washed with acetone, $CHCl_3$, water, 2 M HCl, 2 M NaOH, water, and acetone. The product was then immersed in acetone/$CHCl_3$ (1:1 v/v) for 18 hours, during which the activation solvent was decanted and refreshed twice. After filtration, the product was dried at 120 °C under vacuum (150 mTorr) to give BILP-11 as a brown powder (70 mg, 81%). Anal. Calcd. (%) for $C_{102}H_{63}N_{12}{\cdot}12H_2O$: C, 73.23; H, 5.24; N, 10.05. Found: C, 75.55; H, 4.37; N, 11.00.

Synthesis of BILP-12. BILP-12 was synthesized following the procedure described above for BILP-11 from 2,3,6,7,14,15 hexaaminotriptycene hexahydrochloride salt (65 mg, 0.12 mmol) and TFPPy (50 mg, 0.08 mmol). After drying, the final product BILP-12 was obtained as a yellowish brown fluffy solid (73 mg, 79% yield). Anal. Calcd (%). for $C_{106}H_{67}N_{12}{\cdot}12H_2O$: C, 74.25; H, 5.31; N, 9.80. Found: C, 77.57; H, 4.32; N, 10.35.

Synthesis of BILP-13. BILP-13 was synthesized following the methods mentioned above for BILP-11 and BILP-12 using 3,3` diaminobenzidine tetrahydrochloride salt (58 mg, 0.16 mmol) and TFPPy (50 mg, 0.08 mmol). After drying, the final product BILP-13 was obtained as a brown fluffy solid (67 mg, 75% yield). Anal. Calcd. (%) for $C_{68}H_{46}N_8{\cdot}8H_2O$: C, 72.97; H, 5.58; N,10.01. Found: C, 73.51; H, 4.86; N, 10.09.

3. Results and Discussion

3.1 Synthesis and Characterisation of BILPs

The synthesis of BILPs reported in this study was performed according to the method we reported recently,[15] which is based on acid-catalysed condensation reactions between aryl-*o*-amine and aryl-aldehyde building blocks as depicted in the Fig. 1 Briefly, a solution of TFPPy in DMF was added dropwise to solutions of the corresponding aryl-*o*-diamine building unit dissolved in DMF and stirred for 4 hours at -30 °C. The resulting mixture was stirred under nitrogen at room

Journal of Materials Chemistry A Accepted Manuscript

 This journal is © The Royal Society of Chemistry 2012

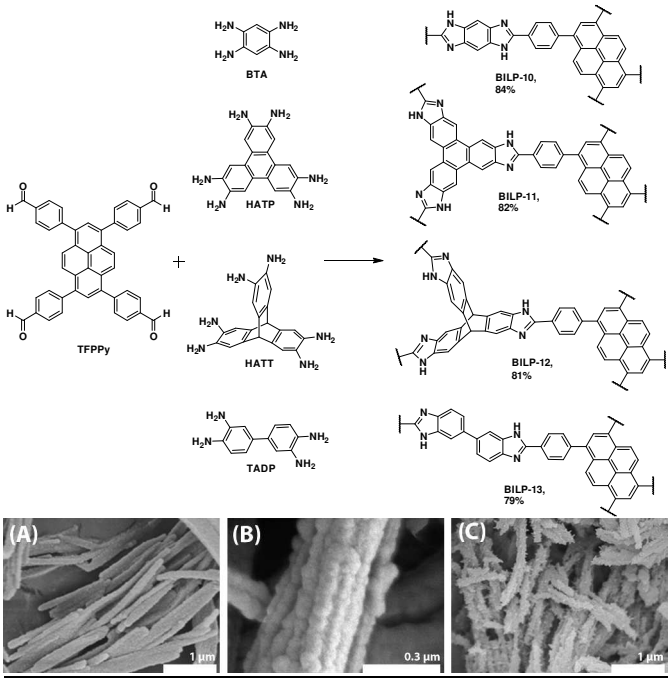

Fig. 1 Synthesis of BILPs, (i) DMF, -30 °C, 3 hr, (ii) DMF, RT, 6 hr under N_2, (iii) DMF, 130 °C, 72 hr under O_2. Scanning electron microscopy (SEM) images of BILP-11 (A), BILP-12 (B) and BILP-13 (C).

temperature to afford an orange suspension, presumably, imine-linked oligomers.[20] Finally, the reaction mixture were gradually heated up to 130 °C in the presence of oxygen and kept for 3 days to afford the corresponding BILP as a yellowish brown suspension. Purification steps involved washing the polymers with 2M aqueous solutions of HCl and NaOH as well as a combination of water, acetone, and chloroform. All polymers are insoluble in common organic solvents such as tetrahydrofuran, DMF, dichloromethane, methanol, and acetone consistent with their expected hypercrosslinked networks. Chemical compositions were confirmed by micro-elemental analysis while thermogravimetric analysis (TGA) of as-prepared BILPs showed initial weight loss of adsorbed water (up to 100 °C) followed by frameworks decomposition at about 400 °C (Fig. S1).

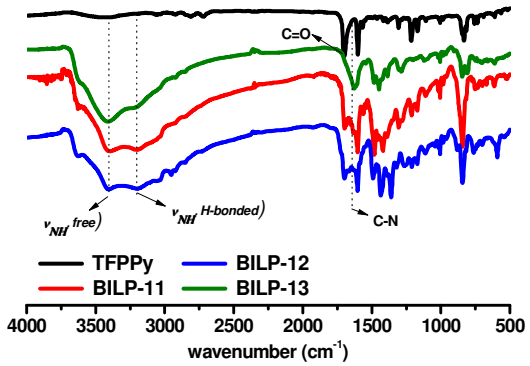

Fig. 2 FT-IR Spectra of TFPPy and BILPs.

The formation of the imidazole ring was verified by FT-IR studies (Fig. 2) which revealed new characteristic stretching bands at 1625 (C=N) 1482 and 1433 cm^{-1} in addition to bands at 3410 and 3180 cm^{-1} for free N-H and hydrogen-bonded N-H, respectively.[15, 21] The consumption of the aldehyde functionality is evidenced by a significant decrease in the intensity of the aldehyde band at 1700 cm^{-1} (C=O). Furthermore, the ^{13}C CP-MAS NMR spectra of BILP-11, BILP-12 and BILP-13 showed N*C*(Ph)N characteristic peaks in the range of 152-153 ppm in line with reported shifts for benzimidazole units in other BILPs.[21, 22] The remaining signals in ^{13}C CP-MAS NMR spectra are assigned to other carbons of the building units (Table S1). The rapid and irreversible imidazole ring formation leads to amorphous polymers according to powder X-ray diffraction (PXRD) studies (Figure S2). Interestingly, based on SEM images (Fig. 1) of all three networks form nanofiber morphologies similar to the pyrene-derived BILP-10. This unique formation of nanofibers is presumably driven by the strong π-π stacking interactions between the pyrene cores, which can assist in solid-state packing of highly porous 2D covalent organic frameworks and thereby enhance gas uptake properties.[17, 23]

3.2 Porosity Studies

The porosity of BILPs was investigated by argon sorption/desorption measurements at 87 K on activated samples (Fig. 3). The fully reversible argon isotherms show rapid argon uptake at low relative pressures (P/P_o < 0.1 bar), which is indicative of their microporous nature.

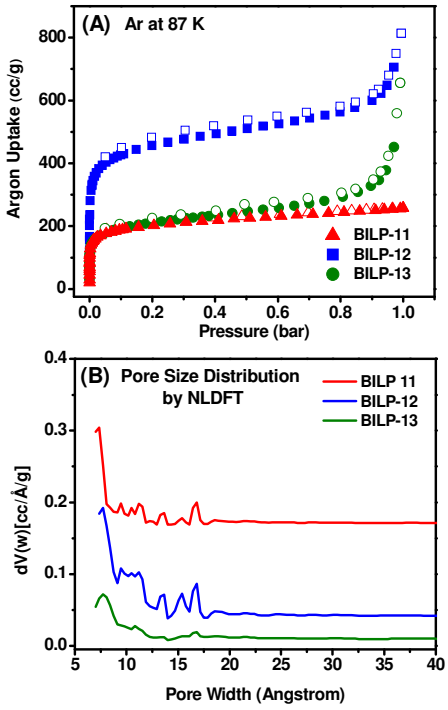

Fig. 3 Argon uptake isotherms at 87 K (A) and pore size distribution from NLDFT (B). Adsorption (filled) and desorption (empty).

Journal of Materials Chemistry A Accepted Manuscript

The isotherms for BILP-12 and BILP-13 show gradual increase in the Ar uptake after P/P_o = 0.90 bar due to argon condensation in interparticle voids. The specific BET surface areas were calculated from the argon sorption branch in the range of P/P_o = 0.05-0.10 bar and found to be 658 m^2 g^{-1} (BILP-11), 1497 m^2 g^{-1} (BILP-12), 677 m^2 g^{-1} (BILP-13). The high surface area of BILP-12 can be attributed to the unique structural features of the triptycene building unit which has high internal molecular free volume (IMFV).[18] Pore size distribution (PSD) was calculated by none-local density functional theory (NLDFT) and gave narrow distributions width maxima in the range of 7.2-7.6 Å (Fig. 3). Pore volumes were calculated at P/P_o = 0.90 and they indicate that BILP-12 (0.76 cc g^{-1}) has a much higher pore volume than BILP-11 (0.32 cc g^{-1}) and BILP-13 (0.42 cc g^{-1}) (Table 2).

Table 2. Porosity properties of pyrene-based BILP calculated from Argon adsorption isotherms measured at 87 K.

Network	S_{BET} ($m^2 g^{-1}$)	$S_{Langmuir}$ ($m^2 g^{-1}$)	V_{total} ($cm^3 g^{-1}$)	Pore size (nm)
BILP-10	787	1039	0.40	0.76
BILP-11	658	813	0.32	0.72
BILP-12	1497	1825	0.76	0.76
BILP-13	677	862	0.42	0.75

It is worth noting that the surface area and pore width values of BILPs are within the desirable range predicted by Wilmer *et. al.* for efficient CO_2 capture and separation processes.[24] Motivated by these observations, we set out to measure the CO_2 uptake and its selective capture over N_2 and CH_4; the major gaseous components in flue gas and methane-rich gases (natural gas and landfill gas), respectively. We collected low pressure sorption isotherms for CO_2, CH_4, and N_2 at 273 K and 298 K to investigate the capture capacity and enthalpies of adsorption (Q_{st}) for CO_2 and CH_4. Both parameters have been identified as key factors in CO_2 separation applications.[12, 25] The CO_2 uptake was significant for BILP-12 (223 mg g^{-1}; 5.06 mmol g^{-1}) at 273 K and 1 bar, competing with the best performing porous organic polymers such as BILP-4 (5.34 mmol g^{-1}),[16] Azo-Linked Polymers (ALPs, 3.52 - 5.37 mmol g^{-1}),[26] hyper-crosslinked polymers HCPs (3.01-3.92 mmol g^{-1}),[27] functionalized conjugated microporous polymers CMPs (1.6–1.8 mmol g^{-1}),[28] porous aromatic frameworks PAFs (3.01-3.92 mmol g^{-1}).[29] On the other hand, BILP-11 and BILP-13 adsorb moderate amounts of CO_2 (136 and 113 mg g^{-1}), respectively.

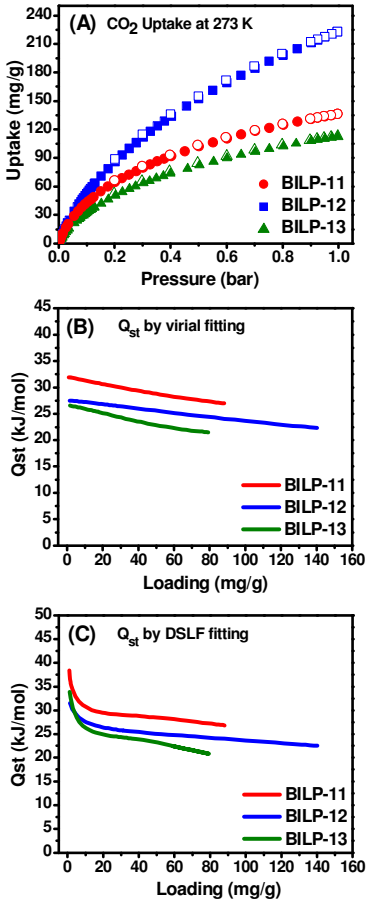

Fig. 4 CO_2 uptake isotherms (A), isosteric heats of adsorption calculated by virial fitting (B) and DSLF fitting (C). Adsorption (filled) and desorption (empty).

Table 3. CO_2 and CH_4 uptakes, isosteric heats of adsorption and selectivity (CO_2/N_2 and CO_2/CH_4) for BILPs

Polymer	[a]CO_2 at 1 bar				[b]CH_4 at 1 bar				[c]Selectivity at 273 K		[c]Selectivity at 298 K		[d]IAST	
	273 K	298 K	Q_{st1}	Q_{st2}	273 K	298 K	Q_{st1}	Q_{st2}	CO_2/N_2	CO_2/CH_4	CO_2/N_2	CO_2/CH_4	CO_2/N_2	CO_2/CH_4
BILP-10	177	111	38.2	38.0	16	11	17.4	20.5	111	14	59	7	57	9.0
BILP-11	136	88	32.0	35.8	16	10	19.0	20.6	103	11	55	7	56	7.6
BILP-12	223	140	27.6	31.2	24	15	18.6	21.7	56	8	31	6	31	6.6
BILP-13	113	79	26.7	32.5	12	9	13.7	16.1	103	9	38	6	32	7.2

[a] Gas uptake in mg g^{-1} and the isosteric enthalpies of adsorption (Q_{st}) in kJ mol^{-1} calculated by virial model (Q_{st1}) reported at zero coverage and DSLF model (Q_{st2}) reported at 0.05 mmol/g loading for CH_4 and 0.04 mmol/g loading for CO_2. [c] Selectivity (mol mol^{-1}) was calculated initial slope method at 273 and 298 K. [d]Selectivity (mol mol^{-1}) was calculated from IAST method at 0.05 bar and 298 K.

Journal of Materials Chemistry A Accepted Manuscript

This journal is © The Royal Society of Chemistry 2012

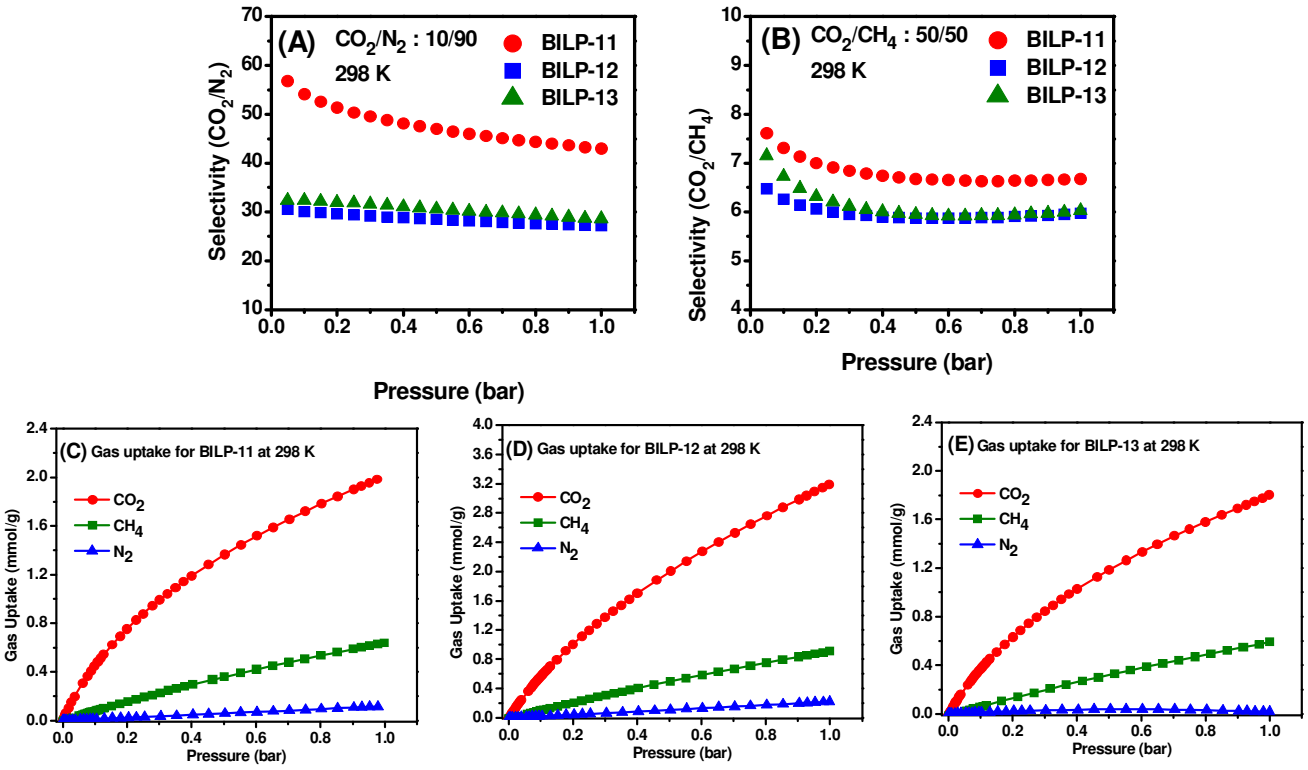

Fig. 5 IAST selectivity of BILPs at 298 K: (A) CO_2/ N_2 (10/90) and (B) CO_2/CH_4 (50/50). Gas uptake for BILPs at 298 K; CO_2 (red circle), CH_4 (olive square), and N_2 (blue triangle).

As stated above, approaching the desirable range for CO_2 binding affinities would be advantageous for selective CO_2 capture and thus, we calculated the Q_{st} for CO_2 from data collected at 273 and 298 K by the virial method and the Clausius-Clapeyron equation as summarized in Table 3 and illustrated in Figure 4. The calculated values indicate that at low coverage, BILPs have strong interaction with CO_2 leading to Q_{st} values in the range of 31.2 to 35.8 kJ mol^{-1}. Such high values were observed because of the narrow pores of BILPs coupled with their N-functionalized pore walls.[30] The Q_{st} drops initially with increased loading and highlights the significance of the CO_2 preferred binding sites, which become less accessible as CO_2 loading increases with pressure increase.[31] BILP-12 has a uniform Q_{st} values over CO_2 loading of 20 to 160 mg g^{-1}. Although the binding affinities are high, all BILPs are easily regenerated by CO_2 desorption through pressure drop as clearly seen from the fully reversible nature of all isotherms at 273 K (Fig. 4A). The CH_4 uptakes at 273 and 298 K and for BILPs revealed a linear correlation with surface area and Q_{st} values (Figure S12).[16] Methane uptakes at 1.0 bar were in the range of 0.78 to 1.47 mmol g^{-1} and as expected, drop to 0.59-0.91 mmol g^{-1} at 298 K. The binding affinities for CH_4 fall in the range of 13.7 to 18.7 kJ mol^{-1}. In contrast to CO_2 and CH_4, the N_2 uptake at 273 K was very low for all polymers (2.17 to 4.00 cc g^{-1}). For all BILPs, CO_2 is the most strongly adsorbed gas when compared to CH_4 and N_2. This is expected as CO_2 has high quadruple moment and polarizability and as hence, it interacts more favourably with polar functionalities present in the pores of BILPs.[32-35]

3.3 CO_2/N_2 and CO_2/CH_4 Selectivity Studies

Once the uptake and binding affinity for CO_2 and CH_4 were established, we investigated the potential use of BILPs in CO_2/N_2 and CO_2/CH_4 separation. The CO_2/N_2 and CO_2/CH_4 selectivities of BILPs were studied by using single-component gas adsorption experiments collected under equilibrium settings. The selectivity of CO_2 over CH_4 and N_2 were calculated by using Henry`s Law which can estimate the initial slope ratios of single-component gas adsorption isotherms at 273 and 298 K (Fig. 4 and Fig. S22).[36]

Initial slope calculations revealed that both BILP-11 and BILP-13 exhibited high selectivity (103) for CO_2 over N_2 at 273 K. As expected, BILP-12 exhibited a lower selectivity (56 at 273 K) confirming the findings of several studies that indicated a trade off between porosity and selectivity levels.[37] In addition to CO_2, high surface area materials with large pores can also accommodate other gas molecules accompanying CO_2 (i.e. N_2 and CH_4), which make the material less effective in gas separation processes. [24, 34, 38]

Besides initial slope calculations, we evaluated the gas mixture adsorption behaviour of BILPs by applying the Ideal Adsorbed Solutions Theory (IAST) wherein selectivity of binary gas mixtures can be predicted by single component adsorption isotherms as a function of pressure. [39]

Journal of Materials Chemistry A Accepted Manuscript

Although the validity of IAST calculations is dependent on the ideality of the polymer,[40] this method has been widely used to investigate amorphous organic polymers such as BILPs,[16] MOPs,[41] POPs,[42] COPs,[43] APOPs,[44] NPOFs,[45] BLP-10(Cl)[46] and azo-COPs[47]. Three main industrial CO_2 capture separation processes; post-combustion flue gas, natural gas and landfill gas were examined to predict the selectivities for CO_2/N_2 and CO_2/CH_4, for gas compositions of 10/90 and 50/50, respectively. Single component adsorption isotherms at 298 K were fitted by either dual-site Langmuir Fruendlich (DSLF) or single-site Langmuir Fruendlich (SSLF) model (Figure S19-24). The IAST selectivity levels are in good agreement with data obtained from initial slope studies (Table 3). In particular, BILP-11 exhibits high CO_2/N_2 and CO_2/CH_4 selectivities of 56 and 7.6 at 298 K, respectively. On the other hand, BILP-12 and BILP-13 show lower CO_2/N_2 (31-32) and CO_2/CH_4 (6.6-7.2) selectivities. The overall trends of high CO_2 uptake and selectivity at ambient conditions encouraged us to evaluate the use of pyrene-based BILPs in CO_2 capture from flue gas, natural gas and landfill gas according to the five criteria suggested by Bae and Snurr.[14] These criteria provide a more comprehensive approach for gauging potential CO_2 adsorbents under PSA and VSA conditions.

3.4 CO_2 Separation from flue gas using VSA

We assessed the potential of all pyrene-based BILPs in CO_2 capture from flue gas (CO_2/N_2 : 10/90) using VSA at 298 K and compared their performance with commercially available activated carbon and zeolites as well as the best performing porous materials in the field as listed in Table 4. The working capacities (ΔN_1) were determined by calculating the CO_2 adsorption difference between 1.0 and 0.1 bar.[14] BILPs showed high working capacities comparable to those of the top performing adsorbents (Table 4). BILP-12 exhibits the highest ΔN_1 (0.49 mol kg^{-1}) followed by BILP-10 (0.41 mol kg^{-1}), BILP-11 (0.38 mol kg^{-1}), and BILP-13 (0.30 mol kg^{-1}). In case of flue gas separation under VSA, the level of CO_2 uptake at 0.1 bar which is influenced by isosteric heat of adsorption of CO_2 can significantly alter the working capacity of adsorbents. For example, BILP-12 has ~90% more specific surface area than BILP-10; however the working capacity of BILP-12 is only ~20% higher than that of BILP-10 due to higher CO_2 binding affinity of latter. For this reason, MOFs that possess open metal cites (*i.e.* Ni-MOF-74) outperform POPs especially at lower CO_2 concentrations.[13]

In addition to high working capacities, all BILPs showed excellent regenerability (R) levels (87.2 to 91) similar to those of ZIF-78 (96.3), ZIF-82 (92.5) and SNU-Cl-va (87.3). Regenerabilities of BILPs surpassed porous Zeolite-13X and Ni-MOF-74, which show higher N_{ads} values than BILPs. However, this trend is associated with much lower regenerability levels (54.2-73.7). Although BILPs have favourable binding sites for CO_2 (imidazole N-sites), their regeneration processes are more favourable than MOFs that have strong interactions between CO_2 and open-metal sites. Another important criterion is the sorbent selection parameter (S), which varies from one BILP to another (72.6 to 157.3). The highest sorbent selection parameter was recorded for BILP-11 (157.3), which can be attributed to its high selectivity factor (α_{12}^{ads} = 42.9).

Table 4. Adsorbents for VSA in flue gas (CO_2/N_2 : 10/90) separation at 298K, P_{ads} = 1 bar and P_{des} = 0.1 bar.

Adsorbents	N_1^{ads}	ΔN_1	R	α_{12}^{ads}	S
BILP-10 [17]	0.45	0.41	90.8	35.5	109.0
BILP-11	0.44	0.38	87.2	42.9	157.3
BILP-12	0.55	0.49	88.7	27.1	72.6
BILP-13	0.34	0.30	89.2	28.6	79.0
Zeolite-13X [14]	2.49	1.35	54.2	86.2	128
SNU-Cl-va[48]	0.47	0.41	87.3	38.0	262
ZIF-78 [14]	0.6	0.58	96.3	34.5	396
ZIF-82 [14]	0.41	0.38	92.5	22.7	101
HKUST-1 [14]	0.62	0.55	89.0	20.4	46.2
Ni-MOF-74 [14]	4.34	3.2	73.7	41.1	83.5
NoritR1 extra[14]	0.38	0.28	73.7	10.7	5.09

3.5 CO_2 Separation from landfill gas using VSA

Landfill gas is an important source of methane gas, however, it usually contains significant levels of CO_2 (CO_2/CH_4 : 50/50) and thus requires processing before transport or use because of the acidic nature of CO_2. Because landfill gas has much higher CO_2 concentration than flue gas or natural gas, the use of the same CO_2 adsorbents may not be always effective in all cases.[13] Therefore, we assessed BILPs performance in landfill gas purification from CO_2 under VSA conditions at 298 K. All polymers showed good working capacity values of 1.44 (BILP-10), 1.11 (BILP-11), 1.71 (BILP-12), and 1.01 (BILP-13) mol kg^{-1}. It is worth noting that the effect of having high surface area becomes more significant as partial pressure of CO_2 increases in gas mixtures. For instance, BILP-12 exhibited ~54% enhancement in working capacity compared to BILP-11, whereas this difference is only ~29% for flue gas case. The working capacities of BILP-10 and BILP-12 exceed those of SNU-Cl-va and ZIF-82 listed in the Table 4. These values indicate that BILPs compete with top adsorbent candidates in field for CO_2 removal form landfill gas by VSA. The regenerability and selectivity factor trends for all BILPs are somewhat similar (81.6–85.3) and (6.0–7.6), respectively, unlike the sorbent selection parameter (S) which varies from 31.8 (BILP-13) to 59.3 (BILP-10). The S value of the latter is very significant but lower than that of SNU-Cl-va (84) and much higher than the levels reported for Mg-MOF-74, ZIF-82, and zeolite-13X (19.1-23.5). Both Mg-MOF-74 and zeolite-13X have higher selectivity factors, however, their regenerability values fall much below those of BILPs.

Journal of Materials Chemistry A Accepted Manuscript

This journal is © The Royal Society of Chemistry 2012

Table 5 Adsorbents for VSA in landfill gas (CO_2/CH_4 : 50/50) separation at 298K, P_{ads} = 1 and P_{des} = 0.1 bars

Adsorbents	N_1^{ads}	ΔN_1	R	α_{12}^{ads}	S
BILP-10 [17]	1.70	1.44	84.3	7.6	59.3
BILP-11	1.36	1.11	81.6	6.7	39.8
BILP-12	2.01	1.71	85.3	6.0	33.7
BILP-13	1.19	1.00	84.2	6.0	31.8
SNU-Cl-va[48]	1.51	1.21	80.6	9.7	84.0
Mg-MOF-74[14]	7.23	2.32	32.1	12.5	23.5
ZIF-82 [14]	1.42	1.2	84.9	5.6	20.5
Zeolite-13X [14]	3.97	1.97	49.6	13.2	19.1
UiO-66-AD6[49]	1.59	1.41	88.5	10	-
NoritR1 extra[14]	1.4	1.17	83.6	2.19	4.5

3.6 CO_2 Separation from natural gas and landfill gas using PSA

Unlike VSA, PSA operates on pressure swing between P_{ads} = 5 bar and P_{des} = 1 bar, therefore, gas uptake measurements were collected in the pressure range of 1.0 to 5.0 bar (Fig. 6A). The PSA working capacities (ΔN_1) of BILPs were determined by CO_2 uptake difference between 5.0 and 1.0 bar. Because high surface area hypothetical MOFs were superior in PSA processes; we anticipated BILP-12 to be more applicable than the other BILPs in both flue gas and landfill gas PSA separation.[13] PSA working capacities of BILP-10, -11, -12 and -13 were found to be 0.80, 0.53, 0.92 and 0.50 mol kg^{-1}, respectively, when natural gas composition (CO_2/CH_4 : 10/90) was considered.

Table 6. Adsorbents for PSA in natural gas (CO_2/CH_4 : 10/90) separation at 298K, P_{ad} = 5 and P_{des} = 1 bars.

Adsorbents	N_1^{ads}	ΔN_1	R	α_{12}^{ads}	S
BILP-10 [17]	1.26	0.80	63.4	8.8	9.3
BILP-11	0.99	0.53	53.7	9.1	6.3
BILP-12	1.52	0.92	60.1	6.0	3.0
BILP-13	0.76	0.50	65.5	5.8	4.2
55%Li red. diimide-POP [14]	1.11	0.63	56.3	16.1	21.4
Zeolite-13X [14]	3.97	1.48	37.3	18.9	9.0
Diimide-POP[14]	1.39	0.86	62.2	9.7	7.5
HKUST-1 [14]	2.7	1.7	63.0	10.0	9.6
Norit R1 extra[14]	1.40	1.02	72.9	4.75	4.0

Landfill gas separation performances of BILPs were also evaluated between 1-5 bar and 298 K. The highest working capacity was observed for BILP-12 (3.02 mol kg^{-1}) for a gas composition of CO_2/CH_4 : 50/50. The other polymers exhibited lower working capacities: BILP-10 (2.18 mol kg^{-1}), BILP-11 (1.31 mol kg^{-1}), and BILP-13 (1.44 mol kg^{-1}). Remarkably, BILP-12 out performs most adorbents in therms of ΔN_1 listed in Table 7 and only exceeded by HKUST-1 (5.34 mol kg^{-1}) and MIL-101 (3.2 mol kg^{-1}). Notably, the working capacities of BILPs are higher for

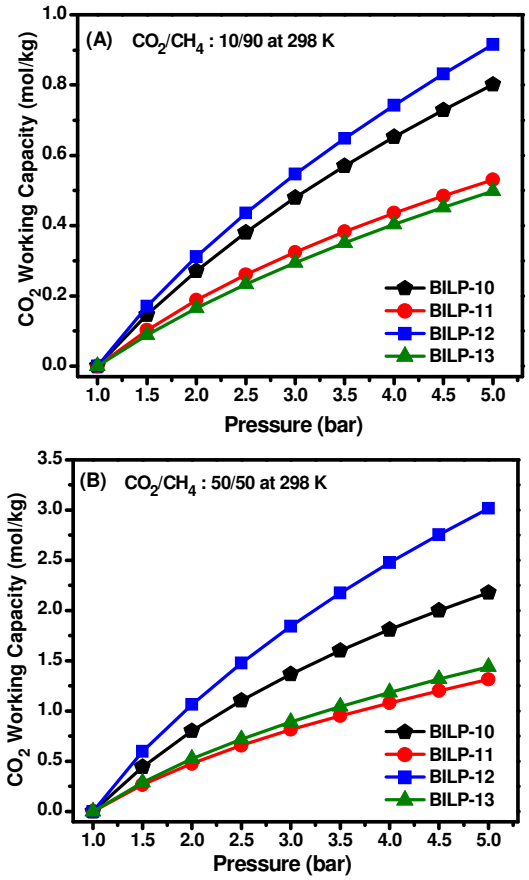

Fig. 6. CO_2 working capacity under PSA conditions for natural gas (A) and landfill gas (B) at 298 K.

landfill gas separation than natural gas separation. This is reasonable because of the high CO_2 content in landfill gas that can reach ~50%. These results suggested that, adsorbents with higher porosity rather effective than their heat of adsorption property at higher CO_2 partial pressures. High pressure CO_2 sorption of BILPs under landfill gas composition showed relevant correlation between ΔN_1 of BILPs and surface area properties. In the case of flue gas, however, CO_2 heats of adsorption and pore size of BILPs were found more related with the ΔN_1 values, most probably, due to low CO_2 composition in the gas mixture (Fig. 6). We also examined other CO_2 capture evaluation criteria such as regenerability and sorbent selection parameters. BILPs exhibited high R values (Table 7). The regenerability of BILP-12 found to be higher than other BILPs. Another important observation is that the α_{12}^{ads} and S parameters of all BILPs exceed those of MOFs and other adsorbents. BILPs resulted in very high S value (29.7-115.3). The remarkable S values of BILPs in general, and BILP-10 in particular, stem from the large difference between the working capacities of pure gas components; CO_2 and CH_4 in this case.[14]

Journal of Materials Chemistry A Accepted Manuscript

Table 7. Adsorbents for PSA in Landfill gas (CO_2/CH_4 : 50/50) separation at 298 K, P_{ads} = 5 bar and P_{des} = 1 bar.

Adsorbents	N_1^{ads}	ΔN_1	R	α_{12}^{ads}	S
BILP-10 [17]	3.84	2.18	56.7	9.6	115.3
BILP-11	2.57	1.31	51.1	7.5	35.3
BILP-12	5.04	3.02	59.8	5.8	29.7
BILP-13	2.51	1.44	57.3	5.6	30.1
Zeolite-13 X [14]	5.37	1.4	26.1	4.2	2.0
HKUST-1 [14]	8.01	5.34	66.7	4.9	21.0
MIL-101 [14]	6.7	3.2	47.8	5	9.5
35% Li-reduced diimide-POP [14]	2.93	1.44	49.2	3.6	11.5
Zn-Atz[50]	3.55	0.63	-	10.63	46.15
MOF-508b [14]	3.6	2.58	71.7	2.9	10.9
Norit R1 extra [14]	3.53	2.13	60.3	2.02	3.58

4.0 Conclusions

In conclusion, we have extended our study on pyrene-derived BILPs by synthesising three new BILPs having enhanced textural properties. The most porous polymer, BILP-12, has pyrene and triptycene building units that lead to high surface area (SA_{BET} = 1497 m^2 g^{-1}) and CO_2 uptake (5.06 mmol g^{-1} at 273 K and 1 bar). The implication of different physical properties (pore size and surface area) on selective CO_2 uptake or separation from N_2 and CH_4 under PSA and VSA were investigated. The IAST data show that BILPs exhibit high CO_2/N_2 selectivity values (32-56 at 298 K). Furthermore, the optimal porosity and CO_2 enthalpy of adsorption render BILP-12 very efficient in landfill and natural gas separation by PSA. On the other hand, the moderate porosities and higher CO_2 binding affinities of BILP-11 and BILP-13 make them better fit for flue gas separation by VSA. Interestingly, the diverse physical properties of BILPs and their N-rich pores enable them to be among the top performing materials for landfill gas and flue gas separation by VSA and PSA. Tailoring such properties within one class of materials has been a challenge especially when chemical stability is not compromised. We are currently investigating the use of BILPs in binary gas mixtures separation under dynamic gas flow.

Acknowledgements

Research supported by the U. S. Department of Energy, Office of Basic Energy Sciences under award number (DE-SC0002576). A. S. thanks Altria for fellowship. T. İ. thanks the Ministry of National Education of Turkey for fellowship.

Notes and references

Department of Chemistry, Virginia Commonwealth University, 1001 W. Main St., Richmond, VA 23284-2006, USA. Fax: (804) 828-8599; Tel.: (804) 828-7505; E-mail: helkaderi@vcu.edu

Electronic Supplementary Information (ESI) available: Spectral characterization of polymers and their gas uptake and selectivity studies. See DOI: 10.1039/b000000x/

1. S. Chu and A. Majumdar, *Nature*, 2012, **488**, 294-303.
2. S. Chu, *Science*, 2009, **325**, 1599-1599.
3. V. Scott, S. Gilfillan, N. Markusson, H. Chalmers and R. S. Haszeldine, *Nat Clim Change*, 2013, **3**, 105-111.
4. J. R. Li, R. J. Kuppler and H. C. Zhou, *Chem. Soc. Rev.*, 2009, **38**, 1477-1504.
5. R. S. Haszeldine, *Science*, 2009, **325**, 1647-1652.
6. D. M. D'alessandro, B. Smit and J. R. Long, *Angew. Chem., Int. Edit.*, 2010, **49**, 6058-6082.
7. K. Sumida, D. L. Rogow, J. A. Mason, T. M. McDonald, E. D. Bloch, Z. R. Herm, T. H. Bae and J. R. Long, *Chem. Rev.*, 2012, **112**, 724-781.
8. Q. Wang, J. Luo, Z. Zhong and A. Borgna, *Energ. Environ. Sci*, 2011, **4**, 42-55.
9. T. C. Drage, C. E. Snape, L. A. Stevens, J. Wood, J. W. Wang, A. I. Cooper, R. Dawson, X. Guo, C. Satterley and R. Irons, *J. Mater. Chem.*, 2012, **22**, 2815-2823.
10. R. Dawson, E. Stockel, J. R. Holst, D. J. Adams and A. I. Cooper, *Energ. Environ. Sci.*, 2011, **4**, 4239-4245.
11. J. A. Mason, K. Sumida, Z. R. Herm, R. Krishna and J. R. Long, *Energ. Environ. Sci.*, 2011, **4**, 3030-3040.
12. P. Z. Li and Y. L. Zhao, *Chem-Asian J*, 2013, **8**, 1680-1691.
13. C. E. Wilmer, O. K. Farha, Y. S. Bae, J. T. Hupp and R. Q. Snurr, *Energ. Environ. Sci.*, 2012, **5**, 9849-9856.
14. Y. S. Bae and R. Q. Snurr, *Angew. Chem., Int. Edit.*, 2011, **50**, 11586-11596.
15. M. G. Rabbani and H. M. El-Kaderi, *Chem. Mater.*, 2011, **23**, 1650-1653.
16. M. G. Rabbani and H. M. El-Kaderi, *Chem. Mater.*, 2012, **24**, 1511-1517.
17. M. G. Rabbani, A. K. Sekizkardes, O. M. El-Kadri, B. R. Kaafarani and H. M. El-Kaderi, *J. Mater. Chem.*, 2012, **22**, 25409-25417.
18. M. G. Rabbani, T. E. Reich, R. M. Kassab, K. T. Jackson and H. M. El-Kaderi, *Chem. Commun.*, 2012, **48**, 1141-1143.
19. S. Q. Ma and H. C. Zhou, *Chem. Commun.*, 2010, **46**, 44-53.
20. E. W. Neuse and M. S. Loonat, *Macromolecules*, 1983, **16**, 128-136.
21. P. Totsatitpaisan, S. P. Nunes, K. Tashiro and S. Chirachanchai, *Solid State Ionics*, 2009, **180**, 738-745.
22. H. Y. Lee, J. Park, M. S. Lah and J. I. Hong, *Chem. Commun.*, 2007, 5013-5015.
23. G. Cheng, T. Hasell, A. Trewin, D. J. Adams and A. I. Cooper, *Angew. Chem., Int. Edit.*, 2012, **51**, 12727-12731.
24. C. E. Wilmer, M. Leaf, C. Y. Lee, O. K. Farha, B. G. Hauser, J. T. Hupp and R. Q. Snurr, *Nat. Chem.*, 2012, **4**, 83-89.
25. Y. H. Xu, S. B. Jin, H. Xu, A. Nagai and D. L. Jiang, *Chem. Soc. Rev.*, 2013, **42**, 8012-8031.
26. P. Arab, M. G. Rabbani, A. K. Sekizkardes, T. İslamoğlu and H. M. El-Kaderi, *Chem. Mater.*, 2014, **26**, 1385-1392.
27. C. F. Martin, E. Stockel, R. Clowes, D. J. Adams, A. I. Cooper, J. J. Pis, F. Rubiera and C. Pevida, *J. Mater. Chem.*, 2011, **21**, 5475-5483.
28. R. Dawson, A. I. Cooper and D. J. Adams, *Polym. Int.*, 2013, **62**, 345-352.
29. T. Ben, C. Y. Pei, D. L. Zhang, J. Xu, F. Deng, X. F. Jing and S. L. Qiu, *Energ. Environ. Sci.*, 2011, **4**, 3991-3999.
30. S. Altarawneh, S. Behera, P. Jena and H. M. El-Kaderi, *Chem. Commun*, 2014, **50**, 3571-3574.
31. Z. Chang, D. S. Zhang, Q. Chen and X. H. Bu, *Phys. Chem. Chem. Phys.*, 2013, **15**, 5430-5442.
32. R. Dawson, D. J. Adams and A. I. Cooper, *Chem. Sci.*, 2011, **2**, 1173-1177.
33. C. Xu and N. Hedin, *J. Mater. Chem. A.*, 2013, **1**, 3406-3414.

Journal of Materials Chemistry A Accepted Manuscript

 This journal is © The Royal Society of Chemistry 2012

34. P. Nugent, Y. Belmabkhout, S. D. Burd, A. J. Cairns, R. Luebke, K. Forrest, T. Pham, S. Q. Ma, B. Space, L. Wojtas, M. Eddaoudi and M. J. Zaworotko, *Nature*, 2013, **495**, 80-84.
35. W. G. Lu, W. M. Verdegaal, J. M. Yu, P. B. Balbuena, H. K. Jeong and H. C. Zhou, *Energ. Environ. Sci.*, 2013, **6**, 3559-3564.
36. J. An, S. J. Geib and N. L. Rosi, *J. Am. Chem. Soc.*, 2010, **132**, 38-39.
37. A. O. Yazaydin, R. Q. Snurr, T. H. Park, K. Koh, J. Liu, M. D. LeVan, A. I. Benin, P. Jakubczak, M. Lanuza, D. B. Galloway, J. J. Low and R. R. Willis, *J. Am. Chem. Soc.*, 2009, **131**, 18198-18199.
38. H. Y. Zhao, Z. Jin, H. M. Su, J. L. Zhang, X. D. Yao, H. J. Zhao and G. S. Zhu, *Chem. Commun.*, 2013, **49**, 2780-2782.
39. A. L. Myers and J. M. Prausnitz, *AICHE J*, 1965, **11**, 121-127.
40. M. Murthi and R. Q. Snurr, *Langmuir*, 2004, **20**, 2489-2497.
41. R. Dawson, T. Ratvijitvech, M. Corker, A. Laybourn, Y. Z. Khimyak, A. I. Cooper and D. J. Adams, *Polym. Chem.*, 2012, **3**, 2034-2038.
42. O. K. Farha, Y. S. Bae, B. G. Hauser, A. M. Spokoyny, R. Q. Snurr, C. A. Mirkin and J. T. Hupp, *Chem. Commun.*, 2010, **46**, 1056-1058.
43. Z. H. Xiang, X. Zhou, C. H. Zhou, S. Zhong, X. He, C. P. Qin and D. P. Cao, *J. Mater. Chem.*, 2012, **22**, 22663-22669.
44. W. C. Song, X. K. Xu, Q. Chen, Z. Z. Zhuang and X. H. Bu, *Polym. Chem.*, 2013, **4**, 4690-4696.
45. T. Islamoglu, M. G. Rabbani and H. M. El-Kaderi, *J. Mater. Chem. A.*, 2013, **1**, 10259-10266.
46. T. E. Reich, S. Behera, K. T. Jackson, P. Jena and H. M. El-Kaderi, *J. Mater. Chem.*, 2012, **22**, 13524-13528.
47. H. A. Patel, S. H. Je, J. Park, D. P. Chen, Y. Jung, C. T. Yavuz and A. Coskun, *Nat. Commun.*, 2013, **4**, 1357.
48. L. H. Xie and M. P. Suh, *Chem-Eur. J.*, 2013, **19**, 11590-11597.
49. D. H. Hong and M. P. Suh, *Chem-Eur. J.*, 2014, **20**, 426-434.
50. I. Erucar and S. Keskin, *Ind. Eng. Chem. Res.*, 2013, **52**, 3462-3472.

Journal of Materials Chemistry A Accepted Manuscript

Table of Content

Pyrene-derived benzimidazole-linked polymers show great promise for CO_2 separation under pressure and vacuum swing adsorption conditions

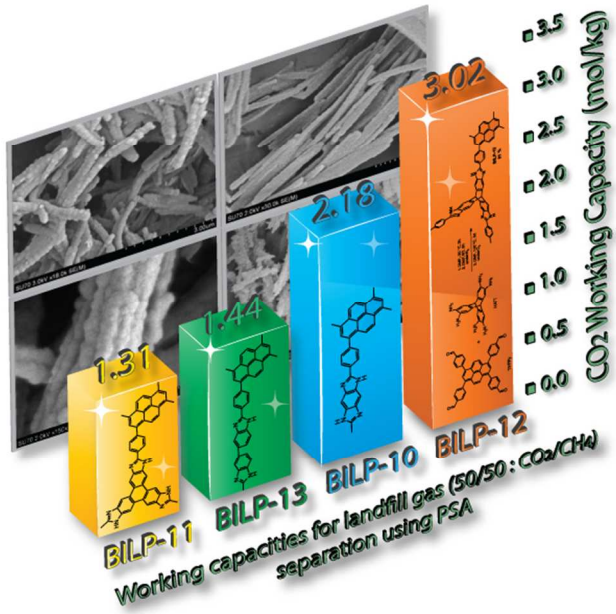

Journal of Materials Chemistry A Accepted Manuscript

This journal is © The Royal Society of Chemistry 2012